Affine Legendre moment invariants for image watermarking robust to geometric distortions.

Hui Zhang, Huazhong Shu, Gouenou Coatrieux, Jie Zhu, Jonathan Q. M. Wu, Yue Zhang, Hongqing Zhu, Limin Luo

HAL Id: inserm-00625194

https://inserm.hal.science/inserm-00625194

Submitted on 21 Sep 2011

Affine Legendre moment invariants for image watermarking robust to geometric distortions

Hui Zhang [1 2] , **Huazhong Shu** [1 2] , **Gouenou Coatrieux** [3] , **Jie Zhu** [1 2] , **Jonathan Q. M. Wu** [4] , **Yue Zhang** [2 1] , **Hongqing Zhu** [5] , **Limin Luo** [2 1 *]

[1] *CRIBS, Centre de Recherche en Information Biomédicale sino-français INSERM : Laboratoire International Associé , Université de Rennes I , SouthEast University , Rennes,FR*

[2] *LIST, Laboratory of Image Science and Technology SouthEast University , Si Pai Lou 2, Nanjing, 210096,CN*

[3] *LATIM, Laboratoire de Traitement de l'Information Medicale INSERM : U650 , Université de Bretagne Occidentale - Brest , Institut Télécom , Télécom Bretagne , CHU Brest , Université européenne de Bretagne , Hopital Morvan, 5 Avenue Foch, 29609 Brest Cedex,FR*

[4] *Department of Electrical and Computer Engineering The University of Windsor , 401 sunset avenue, Windsor, ON N9B3P4,CA*

[5] *Department of Electronics and Communications Engineering East China University of Science and Technology , China meilong road 130, 200237 Shangai, CN*

[*] Correspondence should be adressed to: Limin Luo <luo.list@seu.edu.cn >

Abstract

Geometric distortions are generally simple and effective attacks for many watermarking methods. They can make detection and extraction of the embedded watermark difficult or even impossible by destroying the synchronization between the watermark reader and the embedded watermark. In this paper, we propose a new watermarking approach which allows watermark detection and extraction under affine transformation attacks. The novelty of our approach stands on a set of affine invariants we derived from Legendre moments. Watermark embedding and detection are directly performed on this set of invariants. We also show how these moments can be exploited for estimating the geometric distortion parameters in order to permit watermark extraction. Experimental results show that the proposed watermarking scheme is robust to a wide range of attacks: geometric distortion, filtering, compression, and additive noise.

Author Keywords Affine transformation ; geometric attacks ; image watermarking ; Legendre moment invariants.

Introduction

Image watermarking has been proposed to respond copyright protection concerns [1], [2]. To be efficient, a watermarking scheme must be robust against a wide variety of attacks. Among these attacks, geometric distortions are more difficult to tackle as they affect synchronization between the watermark reader and the embedder.

A number of algorithms robust to rotation, scaling, translation (RST) have been reported in the literature [3]–[8]. Ruanaidh *et al.* [3] utilize the Fourier Mellin transform so that the watermark signal is not impacted by geometric distortions. Image normalization has also been proposed for watermark embedding/extraction in [4]–[7]. In particular, Kim *et al.* [7] watermark Zernike moments of the normalized image. Normalization allows scale and translation invariance while Zernike moments give robustness to rotation. But, as stated by the authors, it seems not possible to watermark directly Zernike moments. They adopt an iterative procedure to construct the watermark from the Zernike moments in the spatial domain in order to control watermark invisibility while imposing specific values to Zernike moments for watermark detection. The resulting watermark is then added to the image pixels. This scheme is public as the original image is not required for detection and has one bit capacity (see [8] for a recent survey). It should be noted that image normalization may increase the computation time and also induce errors in watermark detection/extraction due to image interpolation.

As a general case of RST transformation, affine transformation is more complex. In [9], a template constituted of local peaks at predefined position is embedded in the discrete Fourier transformed image for the purpose of detecting the affine transformation the watermarked image undergone. An invariant watermark proposed by Alghoniemy *et al.* [10] is based on affine geometric moment invariants [11], [12]. They modify moment values of the image so that a predefined function of its geometric moment invariants, a weighted combination of them, lies within a predetermined value. This method is one bit watermarking and public. But, as for [7], a memory and time consuming exhaustive search is necessary to adapt the strength of the watermark, added in the spatial domain, while preserving the output of the predefined function. In fact, moments and moment invariants used in above approaches cannot be watermarked directly. Dong *et al.* [13] exploited geometric moments and the corresponding central moments within an image normalization procedure. The image is normalized so that it meets a set of predefined moment's criteria. The normalized image is consequently invariant to affine geometric transform. This latter is spread spectrum watermarked before being denormalized. This scheme is public and allows multi-bit watermarking but, as above, it may suffer of errors due to image interpolation.

Most of these methods make use of geometric moments which are not orthogonal. However, orthogonal moments are better in terms of image description and are more robust to noise [14]–[17]. Consequently, it can be expected that a set of affine invariants derived from orthogonal moments will offer better performance in terms of robustness, and allows direct watermarking of invariants avoiding thus iterative embedding. Although the orthogonal moments including pseudo-Zernike moments, Tchebichef moments and Krawtchouk moments have been already used to image watermarking [18]–[20], none of them takes the affine transformation into consideration.

In this paper, we present a new method robust to geometric distortion. It is based on a set of orthogonal Legendre moment invariants we propose. The rest of this paper is organized as follows. Section II reviews the definition of Legendre moments and presents our set of invariants to image affine transformation. Watermark embedding, detection, and extraction processes are given in Section III. Before concluding, experimental results are provided in Section IV. They illustrate the overall performance of our approach.

Affine Legendre Moment Invariants

Legendre Moments Definition

The 2-D $(p + q)$th-order Legendre moment of an image function $f(x, y)$ is defined as [15]

$$L_{pq}^{(f)} = \int_{-1}^{1}\int_{-1}^{1} P_p(x)P_q(y)f(x, y)dxdy, \quad p, q = 0, 1, 2 \ldots$$

where $P_p(x)$ is the pth-order orthonormal Legendre polynomial given by

$$P_p(x) = \sum_{k=0}^{p} c_{p,k}x^k$$

with

$$c_{p,k} = \begin{cases} \sqrt{\dfrac{2p+1}{2}}\dfrac{(-1)^{\frac{p-k}{2}}(p+k)!}{2^p\left(\frac{p-k}{2}\right)!\left(\frac{p+k}{2}\right)!k!}, & p-k = \text{even} \\ 0 & p-k = \text{odd}. \end{cases}$$

It can be deduced from (2) that

$$x^p = \sum_{k=0}^{p} d_{p,k}P_k(x)$$

where $D_M = (d_{p,k})$, $0 \le k \le p \le M$, is the inverse matrix of the lower triangular matrix $C_M = (c_{p,k})$. The elements of D_M are given by [21]

$$d_{p,k} = \begin{cases} \dfrac{\sqrt{\frac{2}{2k+1}}2^{\frac{3k-p}{2}}}{\left(\frac{p-k}{2}\right)!\prod_{j=1}^{(p-k)/2}(2k+2j+1)}\dfrac{p!k!}{(2k)!} & p-k = \text{even} \\ 0 & p-k = \text{odd}. \end{cases}$$

Using the orthogonality property of Legendre moments, the image can be approximately reconstructed from a finite number moments of order up to (M, M) as

$$f(x, y) \approx \sum_{i=0}^{M}\sum_{j=0}^{M} P_i(x)P_j(y)L_{ij}^{(f)}.$$

Legendre Moments of an Affine Transformed Image

In this subsection, we establish the relationship between the Legendre moments of an affine transformed image and those of the original image. The affine transformation can be represented by [22]

$$\begin{pmatrix} x' \\ y' \end{pmatrix} = A\begin{pmatrix} x \\ y \end{pmatrix} + \begin{pmatrix} x_0 \\ y_0 \end{pmatrix}$$

where

$$A = \begin{pmatrix} a_{11} & a_{12} \\ a_{21} & a_{22} \end{pmatrix}$$

is called the homogeneous affine transformation matrix.

Translation invariance can be achieved by locating the origin of the coordinate system to the center of mass of the object such that $L_{01}^{(f)} = L_{10}^{(f)} = 0$. Thus, (x_0, y_0) can be ignored and only the matrix is taken into consideration in the remaining part of this paper. However, this simplification is not valid when considering image cropping attack as the center of mass will change (see Section IV).

The 2-D $(p + q)$ th-order Legendre moment of the affine transformed image $g(x', y')$ is defined by

$$
\begin{aligned}
L_{p,q}^{(g)} &= \int_{-1}^{1}\int_{-1}^{1} P_p(x')P_q(y')g(x', y')dx'\,dy' \\
&= \int_{-1}^{1}\int_{-1}^{1} P_p(a_{11}x + a_{12}y)P_q(a_{21}x + a_{22}y) \times g(a_{11}x + a_{12}y, a_{21}x + a_{22}y) \times d(a_{11}x + a_{12}y)d(a_{21}x + a_{22}y) \\
&= \det(A)\int_{-1}^{1}\int_{-1}^{1} P_p(a_{11}x + a_{12}y) \times P_q(a_{21}x + a_{22}y)f(x, y)dx\,dy
\end{aligned}
$$

where $\det(A)$ denotes the determinant of the matrix A.

We can now link the Legendre moments of the affine transformed image given by (8) with those of the original image. By replacing the variable x by $a_{11}x + a_{12}y$ in (2), we have

$$
\begin{aligned}
P_p(a_{11}x + a_{12}y) &= \sum_{m=0}^{p} c_{p,m}(a_{11}x + a_{12}y)^m \\
&= \sum_{m=0}^{p}\sum_{s=0}^{m}\binom{m}{s}c_{p,m}a_{11}^s a_{12}^{m-s}x^s y^{m-s}.
\end{aligned}
$$

Similarly

$$
P_q(a_{21}x + a_{22}y) = \sum_{n=0}^{q}\sum_{t=0}^{n}\binom{n}{t}c_{q,n}a_{21}^t a_{22}^{n-t}x^t y^{n-t}.
$$

Substituting (9) and (10) into (8) yields

$$
L_{p,q}^{(g)} = \det(A)\int_{-1}^{1}\int_{-1}^{1}\sum_{m=0}^{p}\sum_{s=0}^{m}\sum_{n=0}^{q}\sum_{t=0}^{n}\binom{m}{s}\binom{n}{t}c_{p,m} \times c_{q,n}a_{11}^s a_{12}^{m-s}a_{21}^t a_{22}^{n-t}x^{s+t}y^{m+n-s-t}f(x, y)dxdy.
$$

Using (4), we have

$$
\begin{aligned}
x^{s+t} &= \sum_{i=0}^{s+t}d_{s+t,i}P_i(x) \\
y^{m+n-s-t} &= \sum_{j=0}^{m+n-s-t}d_{m+n-s-t,j}P_j(y).
\end{aligned}
$$

Substitution of (12) into (11) leads to

$$
L_{pq}^{(g)} = \det(A)\sum_{m=0}^{p}\sum_{n=0}^{q}\sum_{s=0}^{m}\sum_{t=0}^{n}\sum_{i=0}^{s+t}\sum_{j=0}^{m+n-s-t}\binom{m}{s}\binom{n}{t} \times (a_{11})^s(a_{12})^{m-s}(a_{21})^t(a_{22})^{n-t}c_{p,m}c_{q,n}d_{s+t,i}d_{m+n-s-t,j}L_{ij}^{(f)}.
$$

Equation (13) shows that one Legendre moment of the transformed image is a linear combination of those of the original image.

Affine Legendre Moment Invariants (ALMIs)

Using (13), we can derive a set of ALMIs but its direct use leads to a complex nonlinear system of equations. To reduce complexity, we decompose the matrix into a product of simple matrices. Two kinds of decomposition known as XSR and XYS decompositions can be used [22], [23]. In this work, we adopt the XYS decomposition, which consists in decomposing the affine matrix A into an x-shearing, a y-shearing and an anisotropic scaling matrix, that is

$$
\begin{bmatrix} a_{11} & a_{12} \\ a_{21} & a_{22} \end{bmatrix} = \begin{bmatrix} \alpha_0 & 0 \\ 0 & \delta_0 \end{bmatrix}\begin{bmatrix} 1 & 0 \\ \gamma_0 & 1 \end{bmatrix}\begin{bmatrix} 1 & \beta_0 \\ 0 & 1 \end{bmatrix}
$$

where the coefficients α_0, δ_0, γ_0, and β_0 are real numbers.

Based on this decomposition and using (13), we derive through the following theorems a first set of Legendre moment invariants I_{pq}^{xsh}, I_{pq}^{ysh} and I_{pq}^{as} that are invariant to x -shearing, y -shearing and anisotropic scaling, respectively.

Theorem 1

Let be an original image and g its x -shearing transformed version such as $g(x, y) = f(x + \beta_0 y, y)$. Then the following $I_{pq}^{xsh(f)}$ are invariant to x -shearing

$$I_{pq}^{xsh(f)} = \sum_{m=0}^{p}\sum_{n=0}^{q}\sum_{s=0}^{m}\sum_{i=0}^{s}\sum_{j=0}^{m+n-s} \binom{m}{s}\beta_f^{m-s} \times c_{p,m} c_{q,n} d_{s,i} d_{m+n-s,j} L_{ij}^{(f)}$$

where β_f is a parameter associated with the image f such that $\beta_f = \beta_g + \beta_0$ The proof of Theorem 1 is given in the appendix .

Theorem 2

Let f be an original image and g its y -shearing transformed version such as $g(x, y) = f(x, \gamma_0 x + y)$. Then the following $I_{pq}^{ysh(f)}$ are invariant to y -shearing:

$$I_{pq}^{ysh(f)} = \sum_{m=0}^{p}\sum_{n=0}^{q}\sum_{t=0}^{n}\sum_{i=0}^{m+n-t}\sum_{j=0} \binom{n}{t}\gamma_f^t \times c_{p,m} c_{q,n} d_{m+t,i} d_{n-t,j} L_{ij}^{(f)}$$

where γ_f is a parameter associated with the image f such that $\gamma_f = \gamma_g + \gamma_0$ Theorem proof is similar to that of Theorem 1 and is omitted here.

Theorem 3

Let f and g be two images having the same shape but distinct scale, i.e., $g(x, y) = f(\alpha_0 x, \delta_0 y)$. Then the following I_{pq}^{as} are invariant to anisotropic scaling

$$I_{pq}^{as(f)} = \sum_{m=0}^{p}\sum_{n=0}^{q}\sum_{i=0}^{m}\sum_{j=0}^{n} \alpha_f^{m+1}\delta_f^{n+1} c_{p,m} c_{q,n} d_{mi} d_{nj} L_{ij}^{(f)}$$

where α_f and δ_f are two parameters associated with the image such that $\alpha_f = \alpha_0 \alpha_g$ and $\delta_f = \delta_0 \delta_g$. Theorem proof is given in the appendix .

Determination of the parameters β_f, γ_f, α_f and δ_f will be discussed in Section II-D.

Notice that we can also derive the following theorem without proof.

Theorem 4

The Legendre moments of an image can be expressed through a linear combination of their invariants as follows:

$$L_{pq}^{(f)} = \sum_{m=0}^{p}\sum_{n=0}^{q}\sum_{s=0}^{m}\sum_{i=0}^{s}\sum_{j=0}^{m+n-s} \binom{m}{s}(-\beta_f)^{m-s} c_{p,m} \times c_{q,n} d_{s,i} d_{m+n-s,j} I_{ij}^{xsh(f)}$$

$$L_{pq}^{(f)} = \sum_{m=0}^{p}\sum_{n=0}^{q}\sum_{t=0}^{n}\sum_{i=0}^{m+t}\sum_{j=0}^{n-t} \binom{n}{t}(-\gamma_f)^t \times c_{p,m} c_{q,n} d_{m+t,i} d_{n-t,j} I_{ij}^{ysh(f)}$$

$$L_{pq}^{(f)} = \sum_{m=0}^{p}\sum_{n=0}^{q}\sum_{i=0}^{m}\sum_{j=0}^{n} \alpha_f^{-(m+1)}\delta_f^{-(n+1)} \times c_{p,m} c_{q,n} d_{mi} d_{nj} I_{ij}^{as(f)}.$$

As we will show in Section III, this last theorem will be of great interest for watermarking as it allows avoiding iterative embedding.

From that standpoint, by combining $I_{pq}^{xsh(f)}$, $I_{pq}^{ysh(f)}$, $I_{pq}^{as(f)}$ that are, respectively, invariant to x -shearing, y -shearing, and anisotropic scaling, we can obtain our set of ALMIs. For an image $f(x, y)$, we use the following process.

• Step 1

x -shearing Legendre moment invariants $I_{pq}^{xsh(f)}$ are calculated by (15), where the Legendre moments $L_{ij}^{(f)}$ are computed with (1).

• Step 2

The combined invariants with respect to x-shearing and y-shearing $I_{pq}^{\text{x-ysh}(f)}$ are computed by (16) where the Legendre moments on the right-hand side of (16) are replaced by $I_{pq}^{\text{xsh}(f)}$ computed in Step 1.

- Step 3

The affine Legendre moment invariants $I_{pq}^{\text{affine}(f)}$ are calculated by (17) where the Legendre moments on the right-hand side of (17) are replaced by $I_{pq}^{\text{x-ysh}(f)}$ computed in Step 2.

Parameter Estimation

As described above, the parameters β_f, γ_f, α_f, and δ_f in (15)–(17) are image dependant. We provide one way for estimating these parameters. Considering an affine transform and its XYS decomposition, by setting $I_{30}^{\text{xsh}(f)} = 0$ in (15), we have

$$L_{03}^{(f)}\beta_f^3 + \frac{\sqrt{105}}{3}L_{12}^{(f)}\beta_f^2 + \frac{\sqrt{105}}{3}L_{21}^{(f)}\beta_f + L_{30}^{(f)} = 0.$$

The parameter β_f can then be determined by solving (21).

From (16), we have

$$I_{11}^{\text{ysh}(f)} = \gamma_f\left(L_{00}^{(f)} + \frac{2}{\sqrt{5}}L_{20}^{(f)}\right) + L_{11}^{(f)}$$

Letting $I_{11}^{\text{ysh}(f)} = 0$, we obtain

$$\gamma_f = -\frac{L_{11}^{(f)}}{L_{00}^{(f)} + 2L_{20}^{(f)}/\sqrt{5}}.$$

Setting $I_{20}^{\text{as}(f)} = I_{02}^{\text{as}(f)} = 1$, we have

$$\alpha_f = \sqrt{\frac{\sqrt{b_f^2 + 4a_f} - b_f}{2a_f}}, \qquad \delta_f = \sqrt{\frac{\sqrt{b_f'^2 + 4a_f'} - b_f'}{2a_f'}}$$

where

$$a_f = \sqrt{\frac{V_f^3}{U_f}}$$

$$b_f = -\frac{\sqrt{5}}{2}L_{00}^{(f)}\sqrt{\frac{V_f}{U_f}}$$

$$a_f' = \sqrt{\frac{U_f^3}{V_f}}$$

$$b_f' = -\frac{\sqrt{5}}{2}L_{00}^{(f)}\sqrt{\frac{U_f}{V_f}}$$

$$U_f = L_{02}^{(f)} + \frac{\sqrt{5}}{2}L_{00}^{(f)}$$

$$V_f = L_{20}^{(f)} + \frac{\sqrt{5}}{2}L_{00}^{(f)}$$

The parameters β_g, γ_g, α_g, and δ_g associated with the transformed image $g(x, y)$ can also be estimated according to (21), (23), and (24). It can be verified that the parameters provided by the above method satisfy the following relationships: $\beta_f = \beta_g + \beta_0$, $\gamma_f = \gamma_g + \gamma_0$, $\alpha_f = \alpha_0\alpha_g$ and $\delta_f = \delta_0\delta_g$, where α_0, δ_0, γ_0, and β_0 are the coefficients of the affine transform applied to f. Based on these relationships, conditions given in theorems 1 to 3 are satisfied. It is worth noting that other choice of parameters can also be made to keep the invariance of (15)–(17) to image transformation. For a detailed discussion on the parameter selection methods, we refer the readers to [23] and [24].

Implementation Strategies

In this section, we describe the different processes for watermark embedding, detection and extraction. Proposed ALMIs can be watermarked directly and in different ways by applying spread spectrum or quantization index modulations. However, in order to conduct a fair comparison with other methods based on image moments, we decided to follow the procedure proposed by Alghoniemy *et al* . [10] for watermark detection. Our embedding procedure differs from their proposal as we can directly watermark image invariants contrarily to [10] where an iterative procedure is adopted.

Watermark Embedding

Herein, watermark embedding is carried out in the Legendre moment invariants directly. To illustrate this, let us take the anisotropic scaling invariants $I_{pq}^{as(f)}$ as an example. The x -shearing, y -shearing and affine Legendre moment invariants $I_{pq}^{xsh(f)}, I_{pq}^{ysh(f)}$ and $I_{pq}^{affine(f)}$ can be treated in a similar way.

As in [10], the watermark is generated from the Legendre moment invariants before being inserted in the invariant domain of the original image. Watermark embedding can be noted as follows

$$I_{pq}^{as(h)} = I_{pq}^{as(f)} + s_{pq} I_{pq}^{as(f)}$$

where $I_{pq}^{as(f)}$ and $I_{pq}^{as(h)}$ denote respectively the anisotropic scaling Legendre moment invariants of the original image f and of its watermarked version h , and s_{pq} are the parameters of strength which are selected to achieve the best tradeoff between robustness and imperceptibility. In general, they are selected in a way such that the peak signal-to-noise ratio (PSNR) between the original image f and the watermarked image h is larger than 40 dB in order to make the watermark invisible. The PSNR between f and h is defined as

$$PSNR = 10 \log_{10} \frac{N^2 [\max_{xy} f(x, y)]^2}{\sum_{x=0}^{N-1} \sum_{y=0}^{N-1} [f(x, y) - h(x, y)]^2}$$

where $N \times N$ is the image size.

In this paper, a simple choice of s_{pq} consists to take $s_{pq} = s$ for any p and q . It should be noticed that the watermark embedding method proposed by Kim *et al.* [7] corresponds to a special case of our method with $s_{31} = s_{42} = s$ and $s_{pq} = 0$ for other value of p and q .

Fig. 1(a) illustrates the watermarking of the reference image Lena [see Fig. 2(a)] using its 210 first image moments and s = 0.0214 for a PSNR of 40 dB. The difference of Figs. 2(a) and 1(a) , i.e., the watermark, is depicted in Fig. 1(b) . Sample values of Fig. 1(b) were multiplied by 50 to enhance the difference.

We can express the watermarked image h as a function of the Legendre moment invariants of the original image. In fact, using (20), (26) can be rewritten as

$$L_{pq}^{(h)} = (1 + s_{pq}) L_{pq}^{(f)}$$

With the help of (6), we have

$$h = f + \sum_{p=0}^{M} \sum_{q=0}^{M} s_{pq} P_p(x) P_q(y) L_{pq}^{(f)} = f + W$$

where M is the maximum moment or moment invariant order used for watermarked embedding, W is the image associated with the watermark. The relationship between s , M and the PSNR is illustrated in Fig. 3 . It can be seen that the PSNR obviously decreases with increasing values of s while the order of moment invariants M exploited for embedding has a little effect on the PSNR.

In this experiment, the embedded watermark is completely dependent on the image without any random component; it can be easily estimated from the watermarked image and removed. Thus the embedded watermark does not provide any security. However, this is only a limitation of this experiment as the watermark can be defined more secretly. In fact, instead of deriving the watermark from the Legendre moment invariants [second term $I_{pq}^{as(f)}$ in (26)], one can use a secret watermark pattern. We illustrate that capability in Section III-C, by adding a logo B to obtain the watermarked image ($h = f + W = f + sB$).

Watermark Detection

Watermark detection aims at determining if the received test image is watermarked or not in order to prove ownership. Herein, we follow the same strategy as Alghoniemy *et al.* [10]. We use the distance between the two sets of moment invariants, i.e., between the ALMIs of the watermarked image and those of the received image as detector. The distance between two images in the feature space is measured by

$$d(t, h) = \frac{|I(t) - I(h)|}{|I(h)|}$$

where $I(t)$ and $I(h)$ correspond to the result of a function I applied to the ALMIs of the received and watermarked images, respectively. As in [10], the function I we retain is the mean function

$$I = \frac{1}{L} \sum_{i=1}^{L} I_i^{\text{affine}}$$

where L is the total number of affine invariants used for detection.

The detection decision is then made by comparing the distance $d(t, h)$ with a predefined threshold d_{th}. If the value of $d(t, h)$ is smaller than d_{th}, the detected watermark is declared authentic; otherwise, it is declared unauthentic. As defined, the original image is not required for the watermark detection but as this later relies on $I(h)$ (i.e., a digest of the watermarked image), this method is one bit watermarking and semi-blind.

Watermark Extraction

The procedure we follow in order to recover the watermark from a received image is given in Fig. 4. For simulating this, we consider that a watermarked image h has been affine attacked becoming a received image t. To sum up, once the watermark detected in t, we estimate the affine transform coefficients α_0, δ_0, γ_0, and β_0. A restored image h' can be derived from t by inverting the estimated transform. One has just to subtract the original image f from h' to get access to the watermark W'. Consequently and contrarily to the detection process, the watermark extraction procedure is private, as it requires the original image.

Coefficients α_0, δ_0, γ_0, and β_0 of the affine transform can be estimated in the following way. Let denote $M(h)$ and $M(t)$ be the parameter matrix associated to h and t, respectively

$$M(h) = \begin{bmatrix} \alpha_h & \alpha_h \beta_h \\ \delta_h \gamma_h & \delta_h(1 + \beta_h \gamma_h) \end{bmatrix}$$
$$M(t) = \begin{bmatrix} \alpha_t & \alpha_t \beta_t \\ \delta_t \gamma_t & \delta_t(1 + \beta_t \gamma_t) \end{bmatrix}$$

$M(h)$ and $M(t)$ parameters can be estimated through the procedure given in Section II-D, by making use of (21)–(25). With these notations, α_0, δ_0, γ_0, and β_0 are directly given by the product $M(h)$ and $M^{-1}(t)$.

Experimental Results

Eight standard gray images of 256×256 pixels shown in Fig. 2 were used to evaluate the performances of our scheme. For these experiments, M was set to 20 (i.e., 210 moments were used for embedding). For the comparison purpose, the same invariants' order was considered in our scheme and the one proposed by Alghoniemy *et al.* for embedding. Furthermore, for both methods, moment invariants of order up to three were used for watermark detection [i.e., $L = 4$ in (31)]. More clearly, I_{00}, I_{21}, I_{12}, and I_{03} were used since $I_{10} = I_{01} = I_{11} = I_{30} = 0$ and $I_{20} = I_{02} = 1$ because of the value we retained for β_f, γ_f, α_f, and δ_f, and [see algorithm of Section II-D—(21)–(25)].

In a first experiment, was set to 0.0214, 0.0192, 0.0189, 0.0198, 0.0192, 0.0237, 0.0179, and 0.0187 for Lena, Cameraman, Woman, Boat, Gold Hill, Bridge, Harbor, and Girl images in order to achieve a PSNR of 40.00, 40.01, 40.02, 40.06, 40.00, 40.01, 40.02, and 40.01 dB, respectively. Parameters of [10] were fixed in order to get equivalent PSNR values. Four types of distortions have been considered: rotation, scaling, additive Gaussian noise and JPEG compression. For image rotation, we apply angles varying from 0 to 120 every 20. For image scaling, we consider scale factor evolving from 0.1 to 0.6 with a step of 0.1. The standard deviation of the Gaussian noise varies from 5 to 30 every 5 for the additive noise attack. The JPEG compression quality factor varies from 10 to 60 with a step of 10. We give the average variation of the distance (30) used in the detection process, i.e., the distance between ALMIs of the watermarked image h and of the received image t, for the eight test images. It can be seen from Fig. 5(a)–(d) that with respect to rotation, scaling, additive Gaussian noise and JPEG compression our ALMIs have a better behavior than the affine geometric moment invariants (AGMIs) adopted by Alghoniemy *et al.* [10]. ALMIs' variability is also smaller than AGMIs. In fact, we achieved an averaged standard deviation of 0.2% for ALMIs against 2.6% for Alghoniemy's method in all these experiments.

Considering the same test image set, we then compare detection performance of our scheme with [10] for different PSNR values and under various attacks including rotation, scaling, affine transformation, median filtering, Gaussian noise, salt and pepper noise, speckle

noise, small random distortions (SRD), JPEG compression, cropping, and histogram equalization. For that purpose, we used stirmark 4.0 [1] and Matlab 7.1. The threshold used to decide whether or not an image is watermarked was set to 0.02. The parameters of the two affine transform attacks given in Table I are $a_{11} = 1.1$, $a_{12} = 0.2$, $a_{21} = 0.1$, $a_{22} = 0.8$, and $a_{11} = -1.2$, $a_{12} = 0.3$, $a_{21} = 0.4$, $a_{22} = -0.6$, respectively. In average on the test image set, s was set to 0.0250, 0.0199, 0.0110, and 0.0088 in order to achieve a PNSR of 38, 40, 45, respectively. Results achieved with both methods are summarized in Table I . Indicated values correspond to the detection rate, i.e., the ratio between the number of correctly detected watermark and the number of tested image; and, the average detection distance for [10] and ALMIs [see (30)] under the attacks described above. It can be seen that the proposed method achieves better results whatever the attack type. However, as [10] our scheme is not robust to cropping and histogram equalization attacks. This may be explained by the fact that: 1) we use the image center of mass as origin of the coordinate system, center of mass usually modified by such kind of modifications (see Section II-A), and 2) changes of the image intensity more or less impact invariants' values.

As shown in Section III-C, once the watermarked is detected, one can estimate the affine transform parameters allowing then the watermark extraction. To illustrate the efficiency of our system in that situation, we use a logo image B as watermark W: $h = f + sB = f + W$, where h , f , and B correspond to the watermarked, the original and the logo images, respectively (see Section III-A). B is of same dimensions than our test images, [see Fig. 6(a)] and was embedded in the four test images shown in Fig. 2(a)–(d) using all image moments ($M = 255$) and s fixed to 0.005. Watermarked images were then attacked by an affine transformation as illustrated in Fig. 6(b)–(e) . Affine coefficients and their estimations based on (21)–(25) are listed in Table II . It can be seen that our method fits well the affine transformation coefficients. Extracted watermarks are shown in Fig. 6(f)–(i) . They are correctly recovered.

Conclusion and Perspectives

The major contribution of this paper relies on two aspects. The first one is the derivation of a set of affine invariants based on Legendre moments. Those invariants can be used for estimating the affine transform coefficients applied to one image. The second one is the use of these affine Legendre moment invariants for watermark embedding, detection and extraction. It was shown that the proposed method is more robust than others based on geometric moments.

One weak point of this algorithm is that the watermark detection is considered as a 1-bit watermarking system since the distance between the affine invariants and the threshold is used. However, the proposed detection approach could be extended to a multi-bit watermarking scheme by making use of spread spectrum techniques for example. This subject is currently under investigation. Another limitation of the proposed algorithm is that it is not robust to image cropping and histogram equalization, a common problem for the moment-based watermark algorithms.

Appendix
Proof of Theorem 1

The Legendre moment invariants of the image intensity function $g(x, y)$ is defined as

$$I_{pq}^{xsh(g)} = \sum_{m=0}^{p}\sum_{n=0}^{q}\sum_{s=0}^{m}\sum_{i=0}^{s}\sum_{j=0}^{m+n-s}\binom{m}{s}\beta_g^{m-s}\times c_{p,m}c_{q,n}d_{s,i}d_{m+n-s,j}L_{ij}^{(g)}.$$

Now we want to prove $I_{pq}^{xsh(g)} = I_{pq}^{xsh(f)}$. To that end, we have

$$I_{pq}^{xsh(g)} - I_{pq}^{xsh(f)} = \sum_{m=0}^{p}\sum_{n=0}^{q}\sum_{s=0}^{m}\sum_{i=0}^{s}\sum_{j=0}^{m+n-s}\binom{m}{s}\beta_g^{m-s}$$
$$\times c_{p,m}c_{q,n}d_{s,i}d_{m+n-s,j}L_{ij}^{(g)}$$
$$-\sum_{m=0}^{p}\sum_{n=0}^{q}\sum_{s=0}^{m}\sum_{i=0}^{s}\sum_{j=0}^{m+n-s}\binom{m}{s}\beta_f^{m-s}$$
$$\times c_{p,m}c_{q,n}d_{s,i}d_{m+n-s,j}L_{ij}^{(f)}.$$

From (13), we have

$$L_{ij}^{(g)} = \sum_{m=0}^{i} \sum_{n=0}^{j} \sum_{s=0}^{m} \sum_{i'=0}^{s} \sum_{j'=0}^{m+n-s} \binom{m}{s} \beta_0^{m-s} \times c_{i,m} c_{j,n} d_{s,i'} d_{m+n-s,j'} L_{i'j'}^{(f)}$$

$$= \sum_{i'=0}^{i} \sum_{j'=0}^{i+j-i'} L_{i'j'}^{(f)} S(i, j, i', j', \beta_0)$$

where

$$S(i, j, i', j', \beta_0) = \sum_{m=0}^{i} \sum_{n=0}^{j} \sum_{s=0}^{m} \binom{m}{s} \beta_0^{m-s} c_{i,m} c_{j,n} d_{s,i'} d_{m+n-s,j'}$$

$$= \sum_{m=0}^{i} \sum_{n=0}^{j} \sum_{s=0}^{m} \binom{m}{s} \beta_0^{s} c_{i,m} c_{j,n} d_{m-s,i'} d_{n+s,j'}.$$

Substitution of (A3) into (A2) yields

$$I_{pq}^{xsh(g)} - I_{pq}^{xsh(f)} = \sum_{i=0}^{p} \sum_{j=0}^{p+q-i} \sum_{i'=0}^{i} \sum_{j'=0}^{i+j-i'} L_{i'j'}^{(f)} S(i, j, i', j', \beta_0) \times S(p, q, i, j, \beta_g) - \sum_{i=0}^{p} \sum_{j=0}^{p+q-i} L_{ij}^{(f)} S(p, q, i, j, \beta_f)$$

$$= \sum_{i'=0}^{p} \sum_{j'=0}^{p+q-i'} L_{i'j'}^{(f)} \sum_{i=i'}^{p} \sum_{j=i+j'-i'}^{p+q-i} S(i, j, i', j', \beta_0) \times S(p, q, i, j, \beta_g) - \sum_{i=0}^{p} \sum_{j=0}^{p+q-i} L_{ij}^{(f)} S(p, q, i, j, \beta_f)$$

$$= \sum_{i=0}^{p} \sum_{j=0}^{p+q-i} L_{ij}^{(f)} \left[\sum_{i'=i}^{p} \sum_{j'=i+j-i'}^{p+q-i} S(i', j', i, j, \beta_0) \times S(p, q, i', j', \beta_g) - S(p, q, i, j, \beta_f) \right]$$

Note that we have shifted the indices in the last step of (A5). Using (A4), we have

$$\sum_{i'=i}^{p} \sum_{j'=i+j-i'}^{p+q-i'} S(i', j', i, j, \beta_0) S(p, q, i', j', \beta_g)$$

$$= \sum_{i'=i}^{p} \sum_{j'=i+j-i'}^{p+q-i'} \sum_{m=0}^{i'} \sum_{n=0}^{j'} \sum_{s=0}^{m} \binom{m}{s} \beta_0^{s}$$

$$\times c_{i',m} c_{j',n} d_{m-s,i} d_{n+s,j}$$

$$\times \sum_{m=0}^{p} \sum_{n=0}^{q} c_{p,m} c_{q,n} \sum_{s=0}^{m} \binom{m}{s} \beta_g^{s} d_{m-s,i'} d_{n+s,j'}$$

$$= \sum_{m=0}^{p} \sum_{n=0}^{q} c_{p,m} c_{q,n} \sum_{s=0}^{m} \binom{m}{s} \beta_g^{s}$$

$$\times \sum_{i'=i}^{p} \sum_{j'=i+j-i'}^{p+q-i'} \sum_{m=0}^{i'} \sum_{n=0}^{j'} c_{i',m} c_{j',n}$$

$$\times \sum_{s=0}^{m} \binom{m}{s} \beta_0^{s} d_{m-s,i} d_{n+s,j} d_{m-s,i'} d_{n+s,j'}$$

$$= \sum_{m=0}^{p} \sum_{n=0}^{q} c_{p,m} c_{q,n} \sum_{s=0}^{m} \binom{m}{s} \beta_g^{s}$$

$$\times \sum_{m=0}^{p} \sum_{n=0}^{p+q-i} \sum_{s=0}^{m} \binom{m}{s} \beta_0^{s} d_{m-s,i} d_{n+s,j}$$

$$\times \left(\sum_{i'=m}^{p} d_{m-s,i'} c_{i',m} \right) \left(\sum_{j'=n}^{p+q-i} d_{n+s,j'} c_{j',n} \right)$$

Since both C_M and D_M are lower triangular matrices, and D_M is the inverse of matrix C_M, we have

$$\sum_{i=m}^{p} d_{m-s,i} c_{i,m} = \sum_{i=m}^{m-s} d_{m-s,i} c_{i,m}$$

$$= \begin{cases} 1, & \text{if } m = m - s \\ 0, & \text{otherwise} \end{cases}$$

$$\sum_{j=n}^{p+q-i} d_{n+s,j} c_{j,n} = \sum_{j=n}^{n+s} d_{n+s,j} c_{j,n}$$

$$= \begin{cases} 1, & \text{if } n = n + s \\ 0, & \text{otherwise.} \end{cases}$$

Substituting (A7) into (A6) leads to

$$\sum_{i=i}^{p} \sum_{j=i+j-i}^{p+q-i} S(i, j, i, j, \beta_0) S(p, q, i, j, \beta_g) = \sum_{m=0}^{p} \sum_{n=0}^{q} c_{p,m} c_{qn} \sum_{s=0}^{m} \binom{m}{s} \beta_g^s \times \sum_{s=0}^{m-s} \binom{m-s}{s} \beta_0^s d_{m-s-s,i} d_{n+s+s,j}.$$

Using the relationship $\beta_f = \beta_g + \beta_0$, we obtain

$$S(p, q, i, j, \beta_f) = \sum_{m=0}^{p} \sum_{n=0}^{q} c_{p,m} c_{qn} \sum_{s=0}^{m} \sum_{t=0}^{s} \binom{m}{s}\binom{s}{t} \times \beta_g^t \beta_0^{s-t} d_{m-s,i} d_{n+s,j}$$

$$= \sum_{m=0}^{p} \sum_{n=0}^{q} c_{p,m} c_{qn} \sum_{t=0}^{m} \sum_{s=t}^{m} \binom{m}{t} \times \binom{m-t}{s-t} \beta_g^t \beta_0^{s-t} d_{m-s,i} d_{n+s,j}$$

$$= \sum_{m=0}^{p} \sum_{n=0}^{q} c_{p,m} c_{qn} \sum_{s=0}^{m} \binom{m}{s} \beta_g^s \times \sum_{k=0}^{m-s} \binom{m-s}{k} \beta_0^k d_{m-s-k,i} d_{n+s+k,j}$$

$$= \sum_{i=i}^{p} \sum_{j=i+j-i}^{p+q-i} S(i, j, i, j, \beta_0) S(p, q, i, j, \beta_g).$$

It can be deduced from (A9) and (A5) that $I_{pq}^{xsh(g)} = I_{pq}^{xsh(f)}$.

Proof of Theorem 3

From (13), we have

$$L_{pq}^{(g)} = \sum_{m=0}^{p} \sum_{n=0}^{q} \sum_{s=0}^{m} \sum_{t=0}^{n} \sum_{i=0}^{s+t} \sum_{j=0}^{m+n-s-t} \binom{m}{s}\binom{n}{t} \times \alpha_0^{m+1} \delta_0^{n+1} c_{p,m} c_{qn} d_{mi} d_{nj} L_{ij}^{(f)}.$$

Equation (17) can be written in matrix form as

$$\begin{vmatrix} I_{00}^{as(g)} & I_{01}^{as(g)} & \cdots & I_{0q}^{as(g)} \\ I_{10}^{as(g)} & I_{11}^{as(g)} & \cdots & I_{1q}^{as(g)} \\ \vdots & \vdots & \cdots & \vdots \\ I_{p0}^{as(g)} & I_{p1}^{as(g)} & \cdots & I_{pq}^{as(g)} \end{vmatrix} = C_p \mathrm{diag}\left(\alpha_g^1 \ \alpha_g^2 \ \cdots, \ \alpha_g^{(p+1)}\right) \times D_p \begin{vmatrix} L_{00}^g & L_{01}^g & \cdots & L_{0q}^g \\ L_{10}^g & L_{11}^g & \cdots & L_{1q}^g \\ \vdots & \vdots & \cdots & \vdots \\ L_{p0}^g & L_{p1}^g & \cdots & L_{pq}^g \end{vmatrix} \times (D_q)^T \mathrm{diag}\left(\delta_g^1 \ \delta_g^2 \ \cdots, \ \delta_g^{(q+1)}\right)(C_{q}$$

Equation (A10) can also be written in matrix form as

$$\begin{vmatrix} L_{00}^g & L_{01}^g & \cdots & L_{0q}^g \\ L_{10}^g & L_{11}^g & \cdots & L_{1q}^g \\ \vdots & \vdots & \cdots & \vdots \\ L_{p0}^g & L_{p1}^g & \cdots & L_{pq}^g \end{vmatrix} = C_p \mathrm{diag}(\alpha_0^1 \ \alpha_0^2 \ \cdots, \ \alpha_0^{(p+1)}) D_p \times \begin{vmatrix} L_{00}^f & L_{01}^f & \cdots & L_{0q}^f \\ L_{10}^f & L_{11}^f & \cdots & L_{1q}^f \\ \vdots & \vdots & \cdots & \vdots \\ L_{p0}^f & L_{p1}^f & \cdots & L_{pq}^f \end{vmatrix} \times (D_q)^T \mathrm{diag}(\delta_0^1 \ \delta_0^2 \ \cdots, \ \delta_0^{(q+1)})(C_q)^T$$

Substituting (A12) into (A11) and using the relationships $D_p C_p = I_p$, $\alpha_f = \alpha_0 \alpha_g$ and $\delta_f = \delta_0 \delta_g$ where I_p is the p th order identity matrix, we obtain

$$\begin{pmatrix} I_{00}^{as(g)} & I_{01}^{as(g)} & \cdots & I_{0q}^{as(g)} \\ I_{10}^{as(g)} & I_{11}^{as(g)} & \cdots & I_{1q}^{as(g)} \\ \vdots & \vdots & \cdots & \vdots \\ I_{p0}^{as(g)} & I_{p1}^{as(g)} & \cdots & I_{pq}^{as(g)} \end{pmatrix} = C_p \mathrm{diag}(\alpha_f^1 \; \alpha_f^2 \; \cdots, \; \alpha_f^{(p+1)}) D_p \times \begin{pmatrix} L_{00}^{f} & L_{01}^{f} & \cdots & L_{0q}^{f} \\ L_{10}^{f} & L_{11}^{f} & \cdots & L_{1q}^{f} \\ \vdots & \vdots & \cdots & \vdots \\ L_{p0}^{f} & L_{p1}^{f} & \cdots & L_{pq}^{f} \end{pmatrix} (D_q)^T \times \mathrm{diag}(\delta_f^1 \; \delta_f^2 \; \cdots, \; \delta_f^{(q+1)})(C_q$$

$$= \begin{pmatrix} I_{00}^{as(f)} & I_{01}^{as(f)} & \cdots & I_{0q}^{as(f)} \\ I_{10}^{as(f)} & I_{11}^{as(f)} & \cdots & I_{1q}^{as(f)} \\ \vdots & \vdots & \cdots & \vdots \\ I_{p0}^{as(f)} & I_{p1}^{as(f)} & \cdots & I_{pq}^{as(f)} \end{pmatrix}$$

Thus, we have $I_{pq}^{as(f)} = I_{pq}^{as(g)}$.

Footnotes:

[1] [Online]. Available: http://www.petitcolas.net/fabien/watermarking/stirmark/index.html

References:

- 1 . Petitcolas F . Watermarking schemes evaluation . IEEE Signal Process Mag . 17 : (5) 58 - 64 Sep 2000 ;
- 2 . Podilchuk CI , Delp EJ . Digital watermarking: Algorithms and applications . IEEE Signal Process Mag . 18 : (4) 33 - 46 Jul 2001 ;
- 3 . O'Ruanaidh JJK , Pun T . Rotation, scale, and translation invariant spread spectrum digital image watermarking . Signal Process . 66 : (3) 303 - 317 1998 ;
- 4 . Tang CW , Hang HM . A feature-based robust digital image watermarking scheme . IEEE Trans Signal Process . 51 : (4) 950 - 959 Apr 2003 ;
- 5 . Zheng D , Wang S , Zhao J . RST invariant image watermarking algorithm with mathematical modeling and analysis of the watermarking processes . IEEE Trans Image Process . 18 : (5) 1055 - 1068 May 2009 ;
- 6 . Seo JS , Yoo CD . Image watermarking based on invariant regions of scale-space representation . IEEE Trans Signal Process . 54 : (4) 1537 - 1549 Apr 2006 ;
- 7 . Kim HS , Lee HK . Invariant image watermark using Zernike moments . IEEE Trans Circuits Syst Video Technol . 13 : (8) 766 - 775 Aug 2003 ;
- 8 . Zheng D , Liu Y , Zhao J , Saddik AE . A survey of RST invariant image watermarking algorithm . ACM Comput Surv . 39 : (2) 1 - 91 2007 ;
- 9 . Pereira S , Pun T . Robust template matching for affine resistant image watermarks . IEEE Trans Image Process . 9 : (6) 1123 - 1129 Jun 2000 ;
- 10 . Alghoniemy M , Tewfik AH . Geometric invariance in image watermarking . IEEE Trans Image Process . 13 : (2) 145 - 153 Feb 2004 ;
- 11 . Reiss TH . The revised fundamental theorem of moment invariants . IEEE Trans Pattern Anal Mach Intell . 13 : (8) 830 - 834 Aug 1991 ;
- 12 . Flusser J , Suk T . Pattern recognition by affine moment invariants . Pattern Recog . 26 : (1) 167 - 174 1993 ;
- 13 . Dong P , Brankov JG , Galatsanos NP , Yang Y , Davoine F . Digital watermarking robust to geometric distortions . IEEE Trans Image Process . 14 : (12) 2140 - 2150 Dec 2005 ;
- 14 . Teague M . Image analysis via the general theory of moments . J Opt Soc Amer . 70 : (8) 920 - 930 1980 ;
- 15 . Teh CH , Chin RT . On image analysis by the method of moments . IEEE Trans Pattern Anal Mach Intell . 10 : (4) 496 - 513 Jul 1988 ;
- 16 . Shu HZ , Luo LM , Coatrieux JL . Moment-based approaches in image part 1: Basic features . IEEE Eng Med Biol Mag . 26 : (5) 70 - 74 Sep 2007 ;
- 17 . Shu HZ , Luo LM , Coatrieux JL . Moment-based approaches in image part 2: invariance . IEEE Eng Med Biol Mag . 27 : (1) 81 - 83 Jan 2008 ;
- 18 . Xin YQ , Liao S , Pawlak M . Geometrically robust image watermarking via pseudo-Zernike moments . Proc. Canadian Conf. Elect. Comput. Eng. 2004 ; 939 - 942
- 19 . Yap PT , Paramesran R . An image watermarking scheme based on orthogonal moments . Proc. TENCON IEEE Region 10 2005 ; 1 - 4
- 20 . Venkataramana A , Raj PA . Image watermarking using Krawtchouk moments . Proc. Int. Conf. Comput.: Theory Appl. 2007 ; 676 - 680
- 21 . Shu HZ , Zhou J , Han GN , Luo LM , Coatrieux JL . Image reconstruction from limited range projections using orthogonal moments . Pattern Recog . 40 : (2) 670 - 680 2007 ;
- 22 . Rothe I , Susse H , Voss K . The method of normalization to determine invariants . IEEE Trans Pattern Anal Mach Intell . 18 : (4) 366 - 375 Apr 1996 ;
- 23 . Zhang Y , Wen C , Zhang Y , Soh YC . On the choice of consistent canonical form during moment normalization . Pattern Recog Lett . 24 : (16) 3205 - 3215 2003 ;
- 24 . Zhang Y , Wen C , Zhang Y . Estimation of motion parameters from blurred images . Pattern Recog Lett . 21 : (5) 425 - 433 2000 ;

Fig. 1

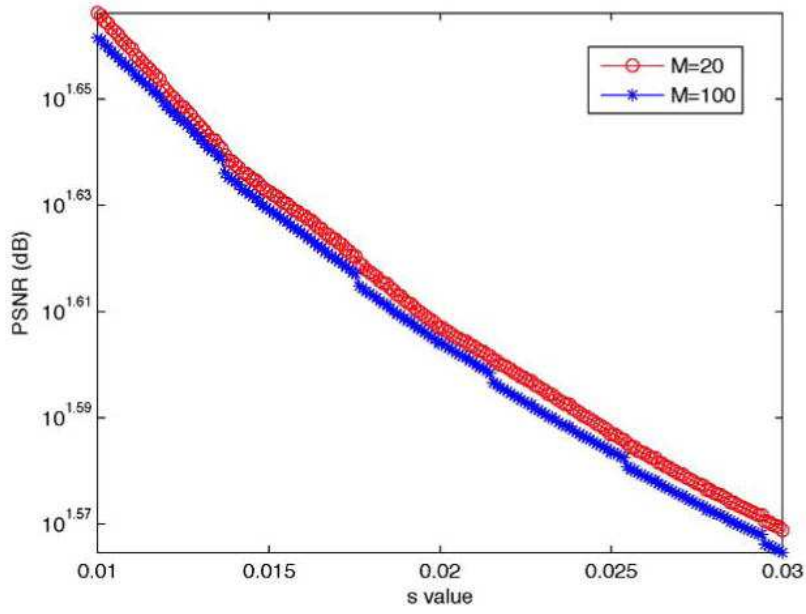(a) Watermarked image with PSNR **=** 40 dB. (b) Magnified watermark.
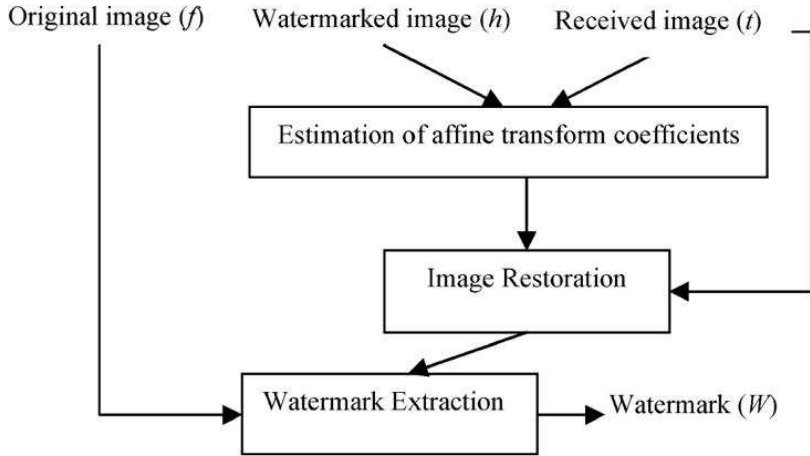

Fig. 2

Original test images.

Fig. 3

PSNR variation for the reference image Lena with respect to the parameter of strength (*s*) and the invariants order (*M*) used for embedding.
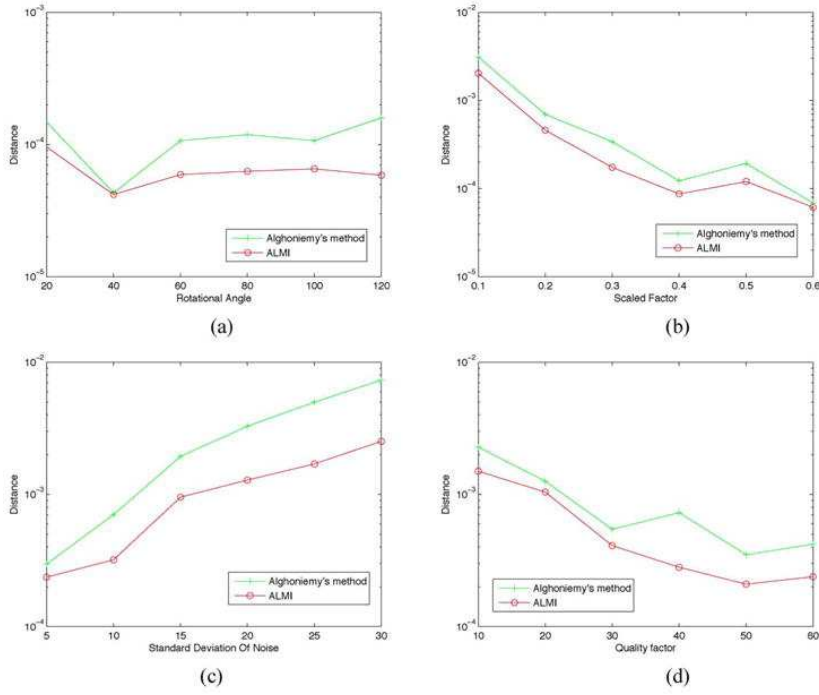

Fig. 4

Watermark extraction procedure.

Fig. 5

Variation in average of the distance between moment invariants with respect to our image test set and different image attacks: (a) rotation attack; (b) scaling attack; (c) gaussian noise attack; (d) JPEG compression attack.

(a)

(b)

(c)

(d)

Fig. 6

(a) Logo used as watermark. (b)–(e) Watermarked images under affine transformation. (f)–(i) Extracted watermark from (b)–(e).

(a)　(b)　(c)　(d)　(e)　(f)　(g)　(h)　(i)
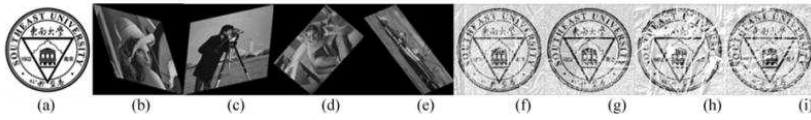
TABLE I

Detection Rate (Det. Rate) and Invariants Distance in Average (Av. Dist.) of Alghoniemy's Method and Our Approach Based on Almis for the Test Image Set Considering Different PSNR Values and After Different Kind of Attacks

	PSNR 38 dB				PSNR 40 dB				PSNR 45dB			
	Av. Dist. [10] (10^{-2})	Av. Dist. ALMIS (10^{-2})	Det. rate [10]	Det. rate ALMIS	Av. Dist. [10] (10^{-2})	Av. Dist. ALMIS (10^{-2})	Det. rate [10]	Det. rate ALMIS	Av. Dist. [10] (10^{-2})	Av. Dist. ALMIS (10^{-2})	Det. rate [10]	Det. rate ALMIS
Affine1	0.084	0.12	1	1	0.083	0.12	1	1	0.086	0.12	1	1
Affine2	0.46	0.37	1	1	0.47	0.37	1	1	0.47	0.37	1	1
Rotation 45°	0.021	0.0096	1	1	0.022	0.010	1	1	0.022	0.0098	1	1
Scaling 0.8	0.052	0.036	1	1	0.051	0.035	1	1	0.051	0.037	1	1
Median filtering	4.67	1.73	0	0.75	4.69	1.74	0	0.75	4.73	1.75	0	0.75
JPEG 20%	0.051	0.070	1	1	0.13	0.10	1	1	0.058	0.066	1	1
Gaussian noise	0.058	0.027	1	1	0.043	0.029	1	1	0.033	0.045	1	1
Salt and pepper noise	0.28	0.20	1	1	0.25	0.21	1	1	0.025	0.015	1	1
Speckle noise	1.47	1.26	0.625	0.75	1.68	1.56	0.625	0.75	1.79	1.72	0.5	0.625
SRD	1.82	0.77	0.625	1	2.33	1.03	0.375	0.875	2.87	1.06	0.25	0.875
Cropping 10%	**48.71**	**18.53**	0	0	**48.64**	**18.59**	0	0	**48.58**	**18.75**	0	0
Histogram equalization	**22.43**	**27.97**	0	0	**23.11**	**28.37**	0	0	**24.51**	**29.52**	0	0

TABLE II

Parameter Estimation Results for the Images Depicted in Fig. 6(b)–(e)

Real transform	$\begin{bmatrix} 1.12 & 0.21 \\ 0.37 & 0.86 \end{bmatrix}$	$\begin{bmatrix} 1.63 & -0.35 \\ -0.14 & 1.38 \end{bmatrix}$	$\begin{bmatrix} -3.56 & 0.62 \\ -2.56 & -0.34 \end{bmatrix}$	$\begin{bmatrix} 1.33 & 0.59 \\ -0.27 & 0.82 \end{bmatrix}$
Estimated parameters	$\begin{bmatrix} 1.1201 & 0.2101 \\ 0.3699 & 0.8600 \end{bmatrix}$	$\begin{bmatrix} 1.6300 & -0.3500 \\ -0.1399 & 1.3800 \end{bmatrix}$	$\begin{bmatrix} -3.5596 & 0.6201 \\ -2.5605 & -0.3399 \end{bmatrix}$	$\begin{bmatrix} 1.33 & 0.59 \\ -0.27 & 0.82 \end{bmatrix}$